A combined size sorting strategy for monodisperse plasmonic nanostructures

Electronic Supplementary Information

Elisabetta Fanizza, [a,b,*] Nicoletta Depalo, [a,b,*] Luciano Clary, [b] Angela Agostiano, [a,b] Marinella Striccoli, [a] M. Lucia Curri [a]

Received (in XXX, XXX) Xth XXXXXXXXX 20XX, Accepted Xth XXXXXXXXX 20XX

DOI: 10.1039/b000000x

1. Optical characterization of Au and Au@SiO_2 nanoparticles. Spectroscopic investigation of the Au nanoparticle (NP) and Au@SiO_2 NP samples are reported in Figure SI1. In particular FT-IR spectra of the core (Figure B-b) and core-shell (Figure C-c) NPs along with that of pure OA (Figure A-a) are reported. Figure 5 D-E shows the UV-Vis absorbance spectra of the nanostructures.

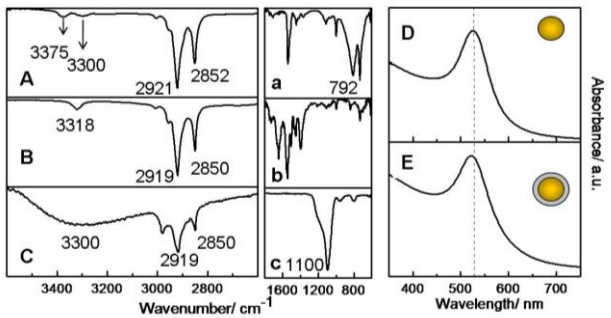

Figure SI1. FTIR spectra in ATR mode of OA (A,a) OA-capped Au NPs (B,b) and silica coated Au NPs (C,c). UV-vis absorbance spectra before (D) and after (E) the growth of the silica shell.

FTIR-spectroscopy in ATR mode on the Au NPs has been performed in order to investigate their surface chemistry, after the purification treatment. The spectrum of the Au NPs (Figure SI 1B-b) has been compared with that of the pure OA (Figure SI 1A-a) and silica coated sample (Figure SI 1C-c). The organic capped Au NP spectrum shows the characteristic vibrational modes of free $-NH_2$ group as a single band at 3318 cm^{-1} instead of the typical double band recorded in the pure OA spectrum (3375 and 3300 cm^{-1}). In addition, in the Au NP spectrum the N-H wagging (792 cm^{-1}) disappears, thus suggesting the coordination of the $-NH_2$ group to the NP surface. Moreover stretching modes characteristic of oxidized $-NH_2$ groups (-CN and imine) can be detected in the spectra (1650 and 1562 cm^{-1}), confirming the OA role as reducing agent, but indicating also as nitrile and imine groups can act as ligands for the NPs. The growth of a silica shell is confirmed by the appearance of an intense peak at 1100 cm^{-1} characteristic of the Si-O-Si network and the presence of silanol OH groups at the silica surface is highlighted by a broad band centred at 3300 cm^{-1}ascribable to the symmetric stretching O-H bond.

In Figure SI 1D-E the UV-Vis absorbance spectra shows the blue shift of the Au plasmon band after the growth of the silica shell. Silica does not exchange charge with the Au NPs), but its refractive index is different from that of both water and ethanol, and also, clearly from that of Au. The growth of a really thin silica shell has no influence in the position of the plasmon band, but at increasing shell thickness a red shift has been observed due to the different dielectric constant of the silica, which turns into a blue shift when the silica shell becomes sufficiently large. Under this condition, scattering becomes significant, resulting in a strong increase in the absorbance at shorter wavelengths. This effect promotes a blue shift of the surface plasmon band and a weakening in the apparent intensity of the plasmon band.

Spectroscopic and morphologic characterization of silica coated Au NPs at increasing precursor concentration. The silica shell growth has been carried out by keeping constant the microemulsion composition, eg. volume of IGEPAL, ammonia solution and Au NP concentration and increasing the volume of injected TEOS (Figure SI2). The TEM micrographs (Figure SI 2D-F) and the statistical analysis (Figure SI 2G) point out an increase in the thickness of the silica shell which results in bead size of 38nm, 45 nm and 101 nm upon TEOS addition of 10 µL, 20 µL and 70 µL, respectively.

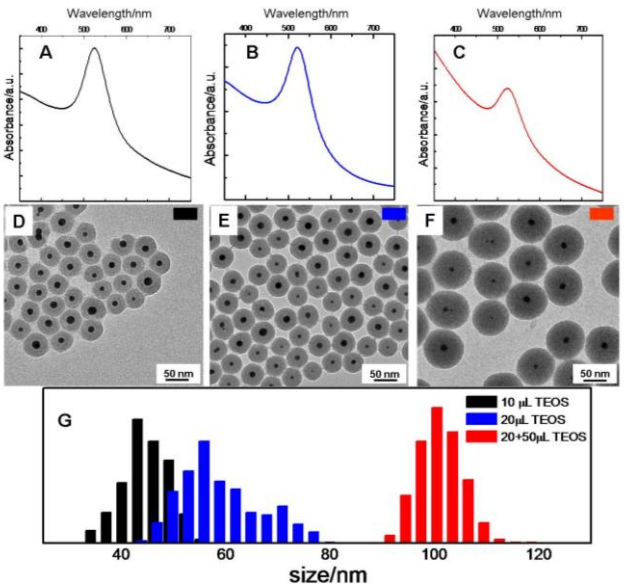

Figure SI 2. UV-Vis absorbance spectra (A-C) and TEM micrographs (D-F) and statistical analysis (G) of Au@SiO_2 NPs prepared at increasing volume of TEOS 10 µL (A, D, black trace), 20 µL (B-E, blue trace) and 70 µL (C, F and red trace).

The change in the position of the SP band (Figure SI 2A-C) agrees with the data reported by Liz Marzan (L. M. Liz-Marzán, M. Giersig, P. Mulvaney *Langmuir*, 1996**, 12**, 4329)

In particular a red shift is detected (525 nm Figure SI 2A) for thin silica shell, a blue shift (523 nm Figure SI 2B) at increased shell thickness and a subsequently shift to lower energy (Figure 525 nm Figure SI 2C) when the shell become much more thicker.

Moreover the core-shell structure size has been found to depend on the Au NP concentration.

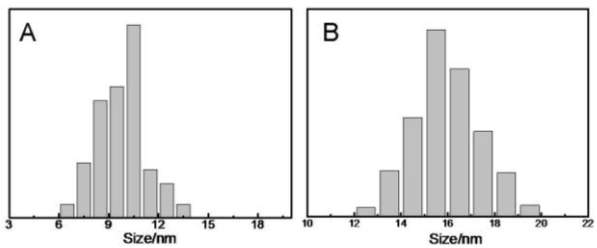

Figure SI 3. Statistical analysis of silica shell thickness for Au@SiO_2 NPs prepared at 4.5*10^{13} NP/mL (A) and 1.3*10^{14} NP/mL (B) Au NP concentration.

A statistical analysis of the shell for core-shell structures prepared at 4.5*10^{13} NP/mL and 1.3*10^{14} NP/mL Au NPs (Figure SI 3) highlights that at lower Au NP concentration, the shell is thinner. In particular shell thickness of nearly 10 nm ($\sigma_{\%}$=9%) and 15nm ($\sigma_{\%}$=9%), respectively, have been measured for Au@SiO_2 nanostructures prepared at 4.5*10^{13} NP/mL and 1.3*10^{14} NP/mL Au NP concentration. This result can be explained by considering that a highr amont of TEOS precursor is used up for the formation of bare SiO_2 NPs, which abundantly nucleate and grow at low Au NP concentration. Therefore less precursor remains available for the growth of the silica shell, which then results thinner at low Au NP concentration.

In addiction an increase in the concentration of Au NPs up to 1.3*10^{14} NP/mL brings to nanostructures with multiple metal NP cores, consistent with a high degree of occupancy of micelles. (Figure SI 4)

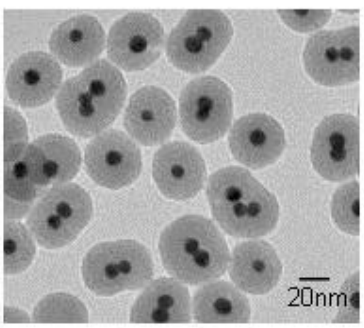

Figure SI 4. TEM micrograph of Au@SiO_2 NPs prepared at Au NP concentration 2*10^{14} NP/mL.

Fabrication of size selected SSAu@SiO_2 NPs.

Three samples of SSAu@SiO_2 NPs have been prepared by using as cores Au NPs collected from the I Fraction (average diameter of 17 nm) II Fraction (average diameter of 11nm), and the III Fraction (average diameter of 7nm) of the as prepared Au NPs. TEM micrographs, showing 25~50 particles, hence statistically representative of the general distribution in the overall samples, have been reported in Figure SI 5.

Similarly, TEM images of the Au@SiO_2 nanostructures collected thanks to the size selection by density gradient centrifugation are shown in Figure SI 6.

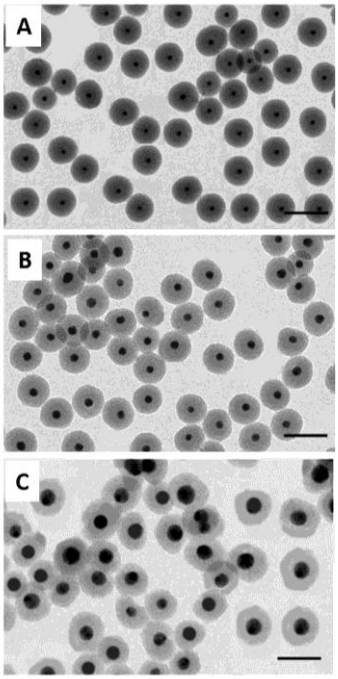

Figure SI 5. TEM images of Au@SiO_2 nanostructures prepared by using size selected Au NP as core: III Fraction (A), II Fraction (B) and I Fraction (C). Scale bar= 50 nm

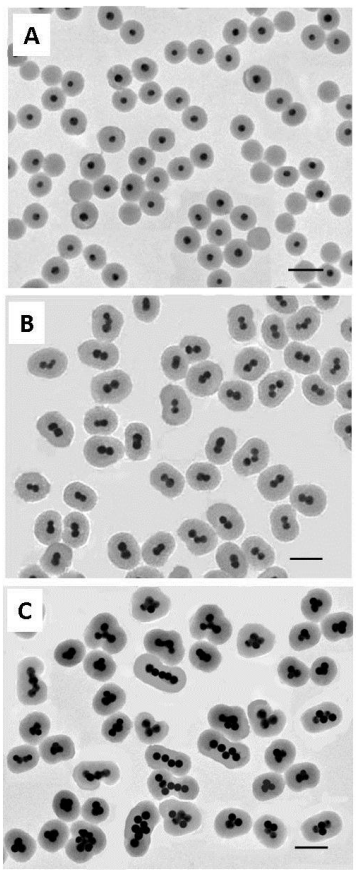

Figure SI 6. TEM micrographs of Au@SiO_2 nanostructures collected by means of density gradient centrifugation. Scale bar= 50 nm